

Supporting Information for

High Performance Chromatographic Characterization of Surface Chemical Heterogeneities of Fluorescent Organic-Inorganic Hybrid Core-Shell Silica Nanoparticles

Thomas C. Gardinier^{1,†}, Ferdinand F.E. Kohle^{2, †}, James S. Peerless³, Kai Ma¹, Melik Z. Turker¹, Joshua A. Hinckley², Yaroslava G. Yingling³, and Ulrich Wiesner^{1,2,*}

Correspondence to: ubw1@cornell.edu

This PDF file includes:

Supplementary Methods
Supplementary References 1-4
Figs. S1 to S11
Tables S1 to S6

Supplementary Methods

High Performance Liquid Chromatography (HPLC).

All HPLC runs were carried out on a Waters Alliance 2965 separations module equipped with a column heater, a Waters 2424 evaporative light scattering detector, and a Waters 2996 photodiode array detector. The sample loop was 50 μL , the standard size for an analytical system. The hardware was controlled by a computer running Empower 3 Feature Release 2 and all chromatograms were analyzed using the ApexTrack peak integration algorithm. Deionized water was generated from a Millipore Milli-Q water system (18.2 $\text{M}\Omega$ resistivity) and acetonitrile was obtained from BDH (UHPLC grade). The columns used were 150 mm Waters Xbridge BEH C4 Protein separation columns with 300 \AA pore size and 3.5 μm particle size. All injections were 8 μL of 15 μM C' dots. Concentrations for injected samples were determined by FCS. The separation method used is as follows: The sample was first injected onto the column in a flow of 90:10 water:acetonitrile at a flow rate of 1 mL/min. These conditions were maintained for 20 minutes to allow equilibration of the analyte with the stationary phase. After 20 minutes the flow rate was slowed to 0.5 mL/min and the baseline was allowed to equilibrate. Then the mobile phase composition was changed to 45:55 water:acetonitrile in a step-like fashion and the baseline was allowed to equilibrate again. Finally a composition gradient of 45:55 to 5:95 water:acetonitrile was carried out for 20 minutes, during this time the analyte elutes from the column. The analytical run above was followed by a short washing step and column equilibration period to ensure that all material from the previous run had eluted from the column and that the column conditions for the next sample analysis were identical to those for the previous sample analysis. In addition to the above method, the same separation method can be used with a constant flow rate of 0.75

mL/minute for the entirety of the experiment for identical results. The use of either method is based entirely on preference, as flow rate changes between 0.5 mL/min and 1 mL/min do not have any drastic effect on the particle separation. The data was collected and analyzed in Empower 3. The ApexTrack integration algorithm native to the Empower 3 software was used to identify peaks and determine the area percentage associated with each eluting peak. For plotting purposes, data was exported after analysis and baseline subtracted with a blank taken before the chromatographic run using OriginLab. For a comparison between baseline subtracted and raw data, see Figure S6.

For the determination of the number of undyed particles in a sample of PEG-Cy5-C' dots it is necessary to use a system of equations based on peak areas from the first and second peaks in both the 647 nm channel and the 275 nm channel. Based on our conclusions regarding the surface chemistry of the nanoparticles eluting in Peak 2, every particle in Peak 2 must contain at least one dye. We assume that the peak area at 275 nm is proportional to the peak area in the 647 nm channel. The number of dyes per particle must also be taken into account when determining the relationship between the two channels, and from after pulse corrected FCS the number of dyes per particle was determined to be 2.0 for Peak 2.

Using this proportionality relationship and the FCS results indicating 1.5 dyes per particle for Peak 1 in the HPLC chromatogram, we can determine from a simple system of equations that approximately 38% of the particles eluted in Peak 1 contain no dye.

Analytical Gel Permeation Chromatography.

Analytical scale gel permeation chromatography was performed on as made solutions prior to preparative scale GPC purification. Injection volumes were 30 μ L of native synthesis solution

diluted with 70 μL of deionized water for a final injection volume of 100 μL . The solution used was the same as the preparative scale GPC solution, prepared the same way directly prior to injection. The column used was a 300 mm Water BioSuite High Resolution Size Exclusion Chromatography column. The separations were performed under isocratic conditions with a flow rate of 1 mL/min. Particle samples including free dye and unreacted PEG-silane eluted within 30 minutes, but the column was run for an additional 20 minutes to ensure that all material had eluted during the chromatographic run.

Dye incorporation efficiency was calculated by using the ApexTrack integration algorithm native to the Empower3 software used to control the instrument and collect data. The peak area percentage attributed to dye at the absorption maximum of the dye is taken to be the percentage of dye successfully incorporated in the nanoparticle.

Fluorescence Correlation Spectroscopy (FCS).

The FCS observation volume V_{eff} was calibrated before each measurement by diluting a dye stock solution with DI water to nanomolar concentrations and determining the structure factor with a standard dye (Alexa Fluor for 635 nm laser and TMR for 532 nm laser). To avoid singlet-triplet transitions in Cy5 dye, all measurements were carried out at 5 kW cm^{-2} . All FCS samples were measured five times in five individual 30 s runs in a 35 mm glass bottom dish (P35G-1.5-10-C, Mattek Corporation) at nanomolar concentration in DI water at 20 °C. The particle diameters, d , were determined from the fits using equation (3) and (4):

$$D = \frac{\omega_{xy}^2}{4\tau_D} \quad (3)$$

$$d = 2 \frac{k_B T}{6\pi\eta D} \quad (4)$$

where D is the diffusion constant, k_B is the Boltzmann's constant, and T is the absolute temperature. Since cis-trans isomerization of co-diffusion Cy5 molecules is independent from each other, the amplitude of isomerization, α , appears smaller, for particles carrying more than one Cy5 molecule. Therefore, P needs to be adjusted for the average number of dyes per particle, n_m , using equations (5) and (6):

$$P = \alpha / (1 + \alpha) \quad (5)$$

$$\alpha = \alpha_P / n_m \quad (6)$$

To determine n_m the measured optical density of each sample was compared to the mean particle concentration as obtained by FCS using equation (7):

$$n_m = \frac{C_{Abs}}{\langle C \rangle_{FCS}} \quad (7)$$

Total Internal Reflection Fluorescence Microscopy (TIRFM).

Samples for photobleaching experiments were prepared by immobilizing biotinylated particles on streptavidin coated glass slides. Streptavidin coated slides were prepared by binding streptavidin via GMBS and MPTMS to a plasma cleaned glass bottom slide (P35G-1.5-14-C, Mattek Corporation) as previously described². Free particles were removed by rinsing the slides with PBS twice before covering the sample with 1 mL of PBS and a glucose oxidase/catalase oxygen scavenger system. Single particle imaging was performed on an inverted Zeiss Elyra microscope operated at TIRF angles of 62–65° as indicated in the Zen 2012 (Zeiss) software, using a 1.46 NA 100X oil immersion objective, and 642 nm laser (laser power 0.165 mW, measured at the

objective) with typical integration times of 100 ms per frame. Fluorescence emission was spectrally filtered with a 655 nm long pass filter. Each movie was recorded at 10 Hz until 99% of the initial fluorescence signal decayed. The excitation laser was turned on right after the photobleaching movie recording was started. The “Definite focus” focal-drift compensation was activated during data acquisition. To avoid overlapping point spread functions only samples that were sparsely labeled with particles were included in the analysis.

Simulations.

All simulations utilized periodic boundary conditions, the Langevin thermostat with a collision frequency of 2 ps^{-1} , the Berendsen barostat (if NPT ensemble) with a relaxation time of 1 ps, and a van der Waals cutoff value of 8 \AA with long-range electrostatics calculated via the Particle Mesh Ewald method. Prior to production simulations, each system was independently equilibrated with the silica surface and dye molecule harmonically restrained with a force constant of 5.0 kcal/mol by the following five-step procedure: (1) structural energy minimization, (2) a constant-volume (NVT ensemble) heating step from 0 to 300 K at a rate of 3 K/ps, (3) an NVT equilibration step at 300 K for 0.3 ns, (4) a constant-pressure (NPT ensemble) equilibration step at 1 atm and 300 K for 0.5 ns, and (5) an NPT equilibration step at 1 atm and 300 K with a timestep of 2 fs and the SHAKE algorithm³ applied to covalent bonds involving a hydrogen for 1 ns (steps 1 to 4 used a 1 fs timestep). Production simulations, from which all reported data was calculated, were performed in the NPT ensemble at 1 atm and 300 K with a timestep of 2 fs for 100 ns. Linear interaction energies were calculated using AMBER’s cpptraj post-processing software⁴.

Supplementary References

1. Chmyrov, V.; Spielmann, T.; Hevekerl, H.; Widengren, J. Trans-Cis Isomerization of Lipophilic Dyes Probing Membrane Microviscosity in Biological Membranes and in Live Cells. *Anal. Chem.* **2015**, *87*, 5690–5697.
2. Kao, T.; Kohle, F. F. E.; Ma, K.; Aubert, T.; Andrievsky, A.; Wiesner, U. Fluorescent Silica Nanoparticles with Well-Separated Intensity Distributions from Batch Reactions. *Nano Lett.* **2018**, *18*, 1305-1310.
3. Ryckaert, J.-P.; Ciccotti, G.; Berendsen, H. J. Numerical Integration of the Cartesian Equations of Motion of a System with Constraints: Molecular Dynamics of n-Alkanes. *J. Comput. Phys.* **1977**, *23*, 327–341.
4. Roe, D. R.; Cheatham III, T. E. PTRAJ and CPPTRAJ: Software for Processing and Analysis of Molecular Dynamics Trajectory Data. *J. Chem. Theory Comput.* **2013**, *9*, 3084–3095.

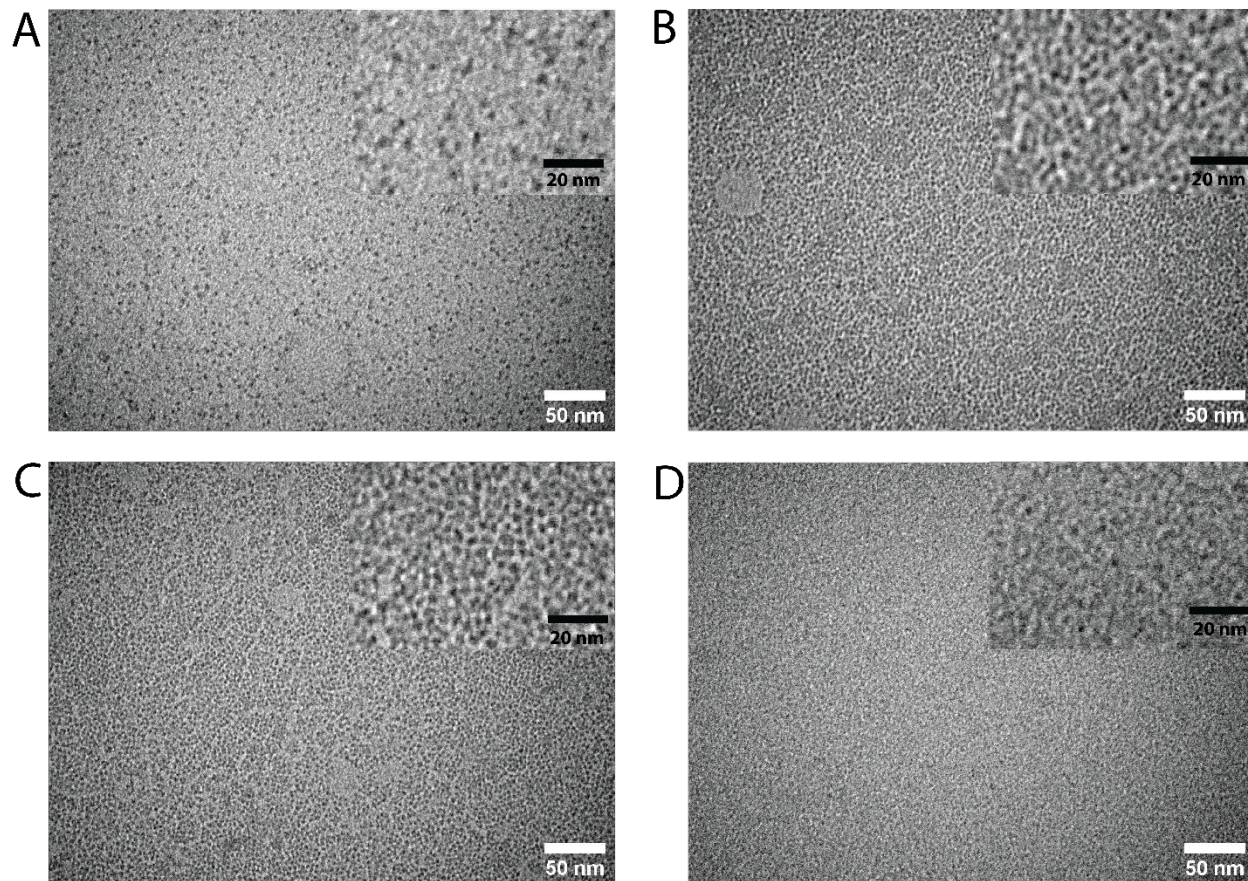


Figure S1: (A-D) Transmission electron microscopy images at two different magnifications (see insets) of particles collected from peaks 1-4 eluted in the HPLC separation as shown in Figure 1B/D of the main text. (A) Peak 1, (B) Peak 2 (the hard sphere diameter as determined by measuring of over 150 nanoparticles was 3.9 nm), (C) Peak 3 (the hard sphere diameter as determined by measuring of over 150 nanoparticles was 3.5 nm), and (D) Peak 4. Please note that as a result of the amount of particles coming out from under the four different HPLC peaks the particle concentration of solutions shown in B and C were highest which is reflected in the TEM images shown here (see corresponding HPLC peak heights in Figure 1B/D of the main text).

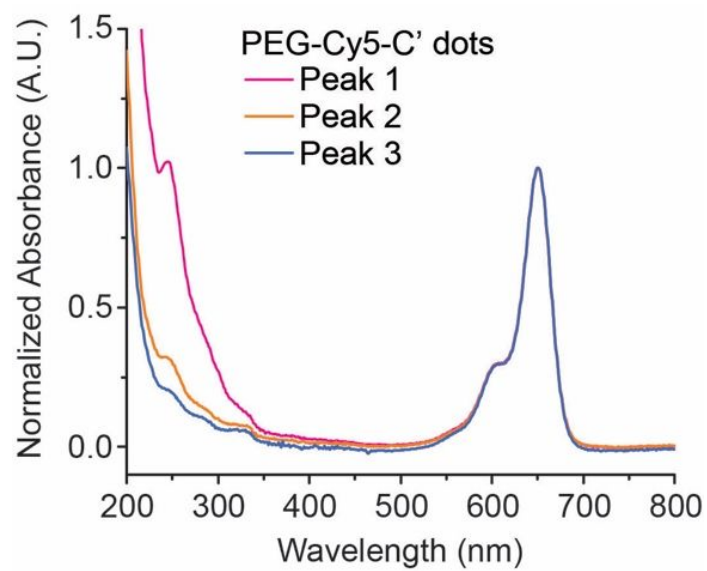


Figure S2: UV/Vis spectra of peak 1 (Pink), peak 2 (Orange), and peak 3 (Blue), collected from HPLC fractionation.

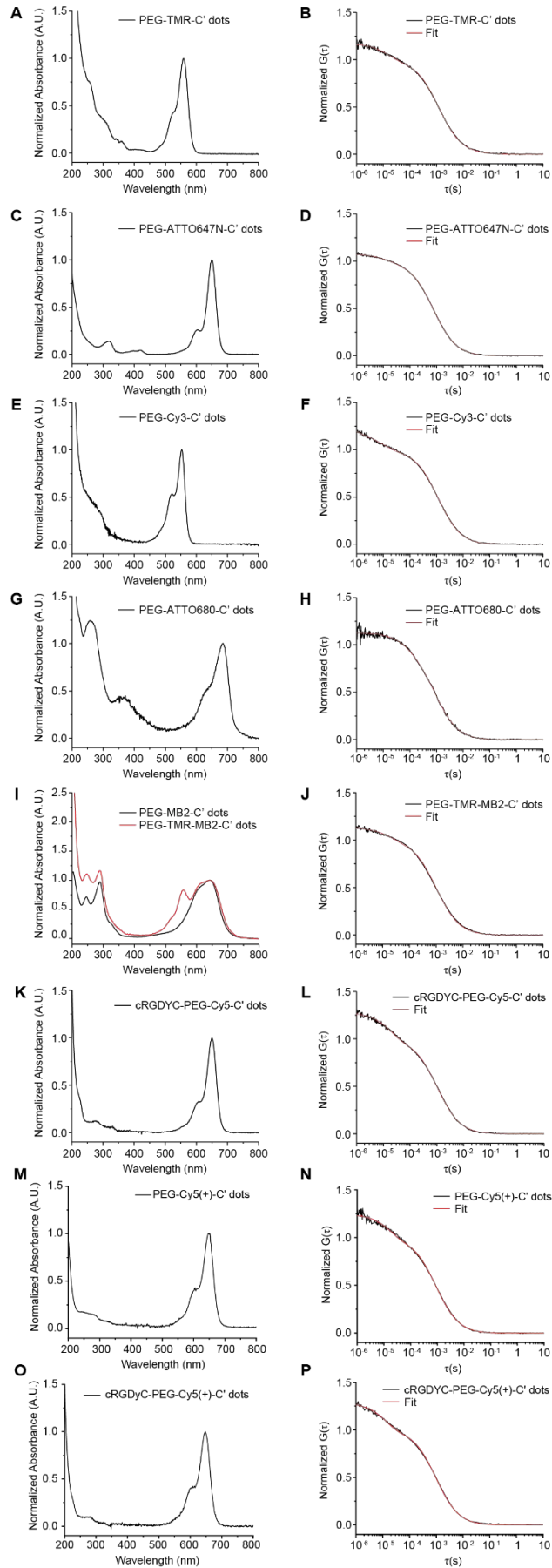


Figure S3: (A) & (B) UV/Vis spectrum and FCS correlation curve of PEG-TMR -C' dots. (C) & (D) UV/Vis spectrum and FCS correlation curve of PEG- ATTO647N -C' dots. (E) & (F) UV/Vis spectrum and FCS correlation curve of PEG-Cy3-C' dots. (G) & (H) UV/Vis spectrum and FCS correlation curve of PEG-ATTO680-C' dots. (I) & (J) UV/Vis spectrum and FCS correlation curve of PEG-TMR-MB2-C' dots. (K) & (L) UV/Vis spectrum and FCS correlation curve of cRGDyC-PEG-Cy5-C' dots. (M) & (N) UV/Vis spectrum and FCS correlation curve of PEG-Cy5(+)-C' dots. (O) & (P) UV/Vis spectrum and FCS correlation curve of cRGDyC-PEG-Cy5(+)-C' dots.

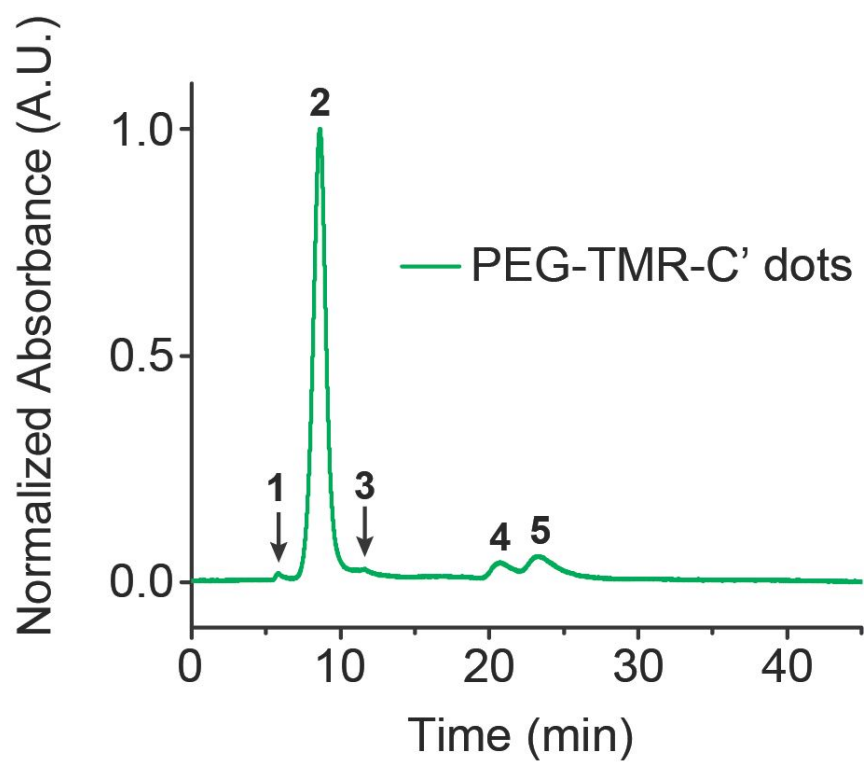


Figure S4: GPC chromatogram of native synthesis solution of PEG-TMR-C' dots collected at 550 nm to measure dye incorporation. Peak labels correspond to Table S2.

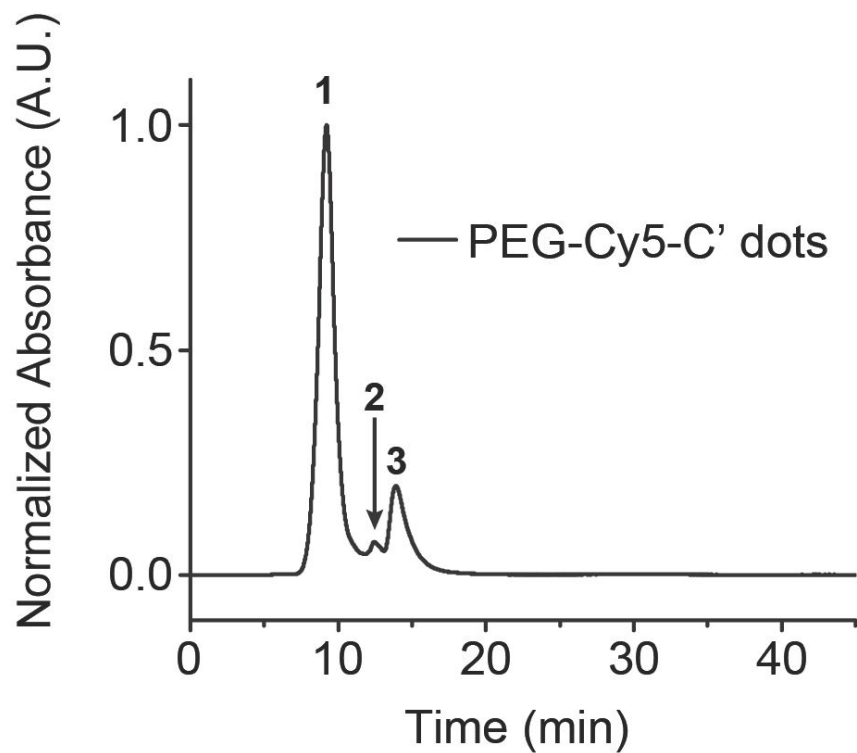


Figure S5: GPC chromatogram of native synthesis solution of PEG-Cy5-C' dots collected at 647nm to measure dye incorporation. Peak labels correspond to Table S3.

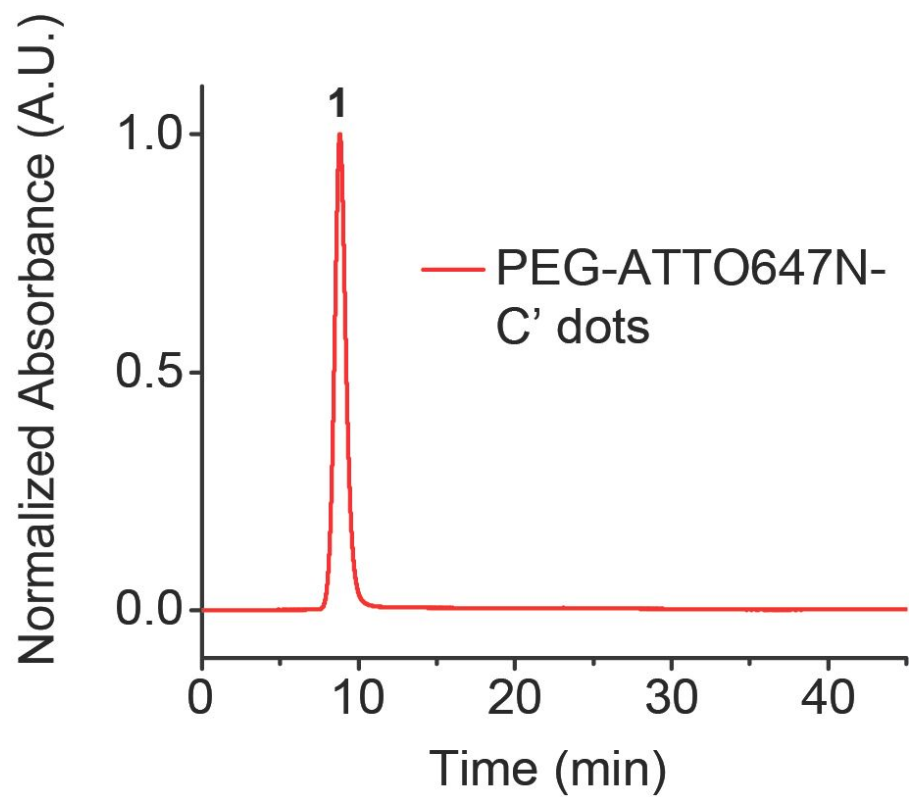


Figure S6: GPC chromatogram of native synthesis solution of PEG-ATTO647N-C' dots collected at 647nm to measure dye incorporation.

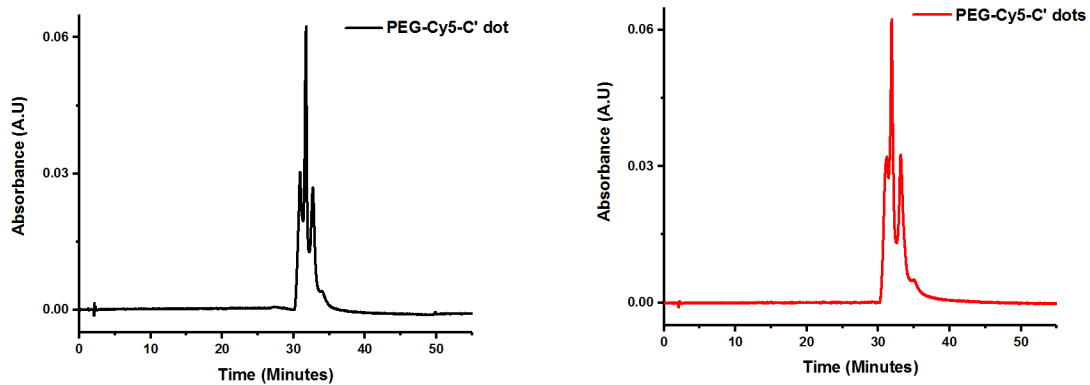


Figure S7: (A) representative chromatogram of PEG-Cy5-C' dots with no post processing done i.e, baseline subtraction, (B) the same chromatogram with baseline subtraction applied.

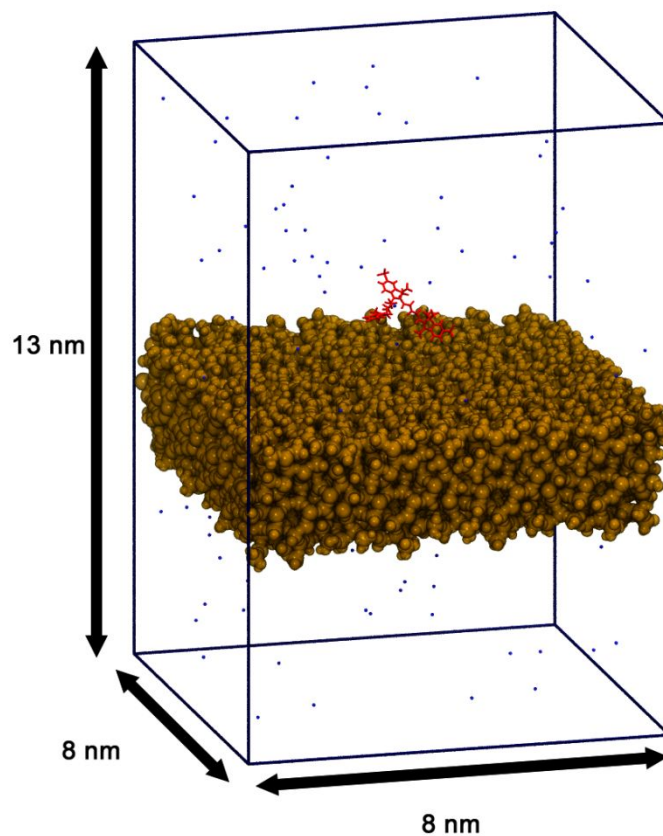


Figure S8: Representative system of silica surface-dye MD simulations as-constructed, composed of water (not shown for clarity), amorphous SiO_2 (brown), Cy5 maleimide (red), and ammonium ions (blue). In other systems, Cy5 maleimide is replaced with the dye of interest, with or without attached silane unit.

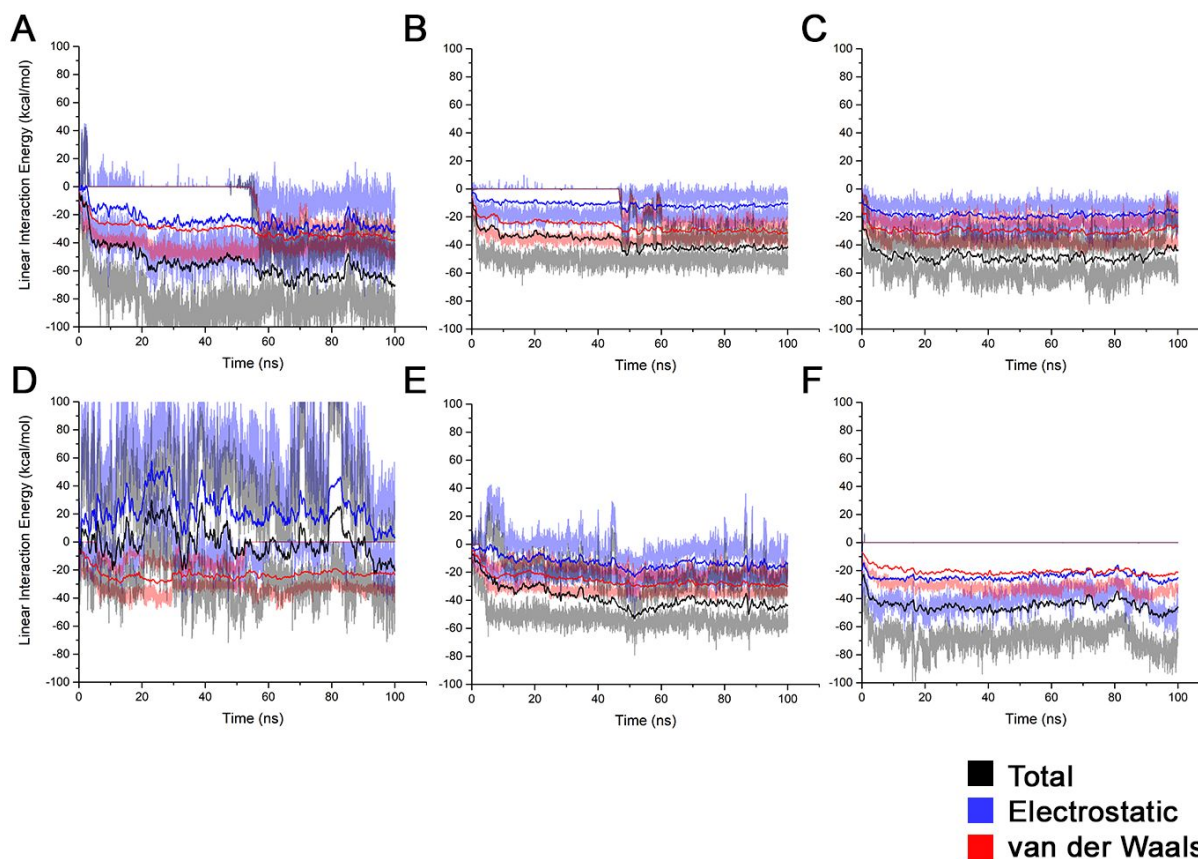


Figure S9 (A-F): Linear interaction energy between silica surface and dye silanes over the entirety of the production simulations. Solid lines denote average of five simulations with random starting dye orientation, transparent lines indicate maximum and minimum of five simulations with random starting dye orientation. (A-C) 1% deprotonated silica surface, (D-F) 15% deprotonated silica surface. (A,D) Cy5, (B,E) TMR, and (C,F) ATTO647N.

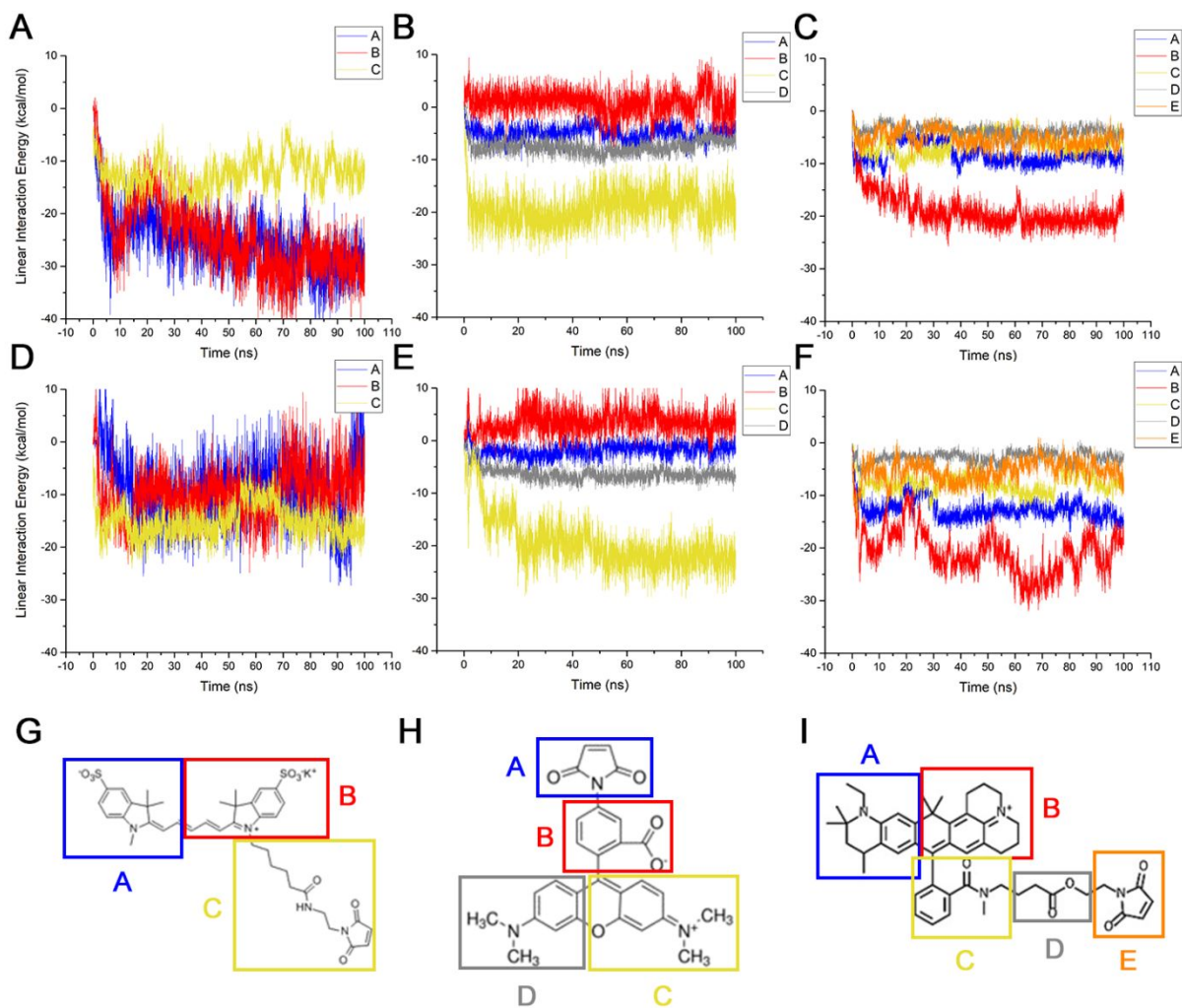


Figure S10: (A-F) Linear interaction energies between silica surface and specific groups of maleimide dye atoms. (A-C) 1% deprotonated silica surface, (D-F) 15% deprotonated silica surface. (A,D) Cy5, (B,E) TMR, and (C,F) ATTO647N. (G-I) Illustrations of atom groupings for Cy5 (G), TMR (H), and ATTO647N (I), respectively. Group interactions highlight how the charged sections of the dye molecule dominate interactions with the silica surface.

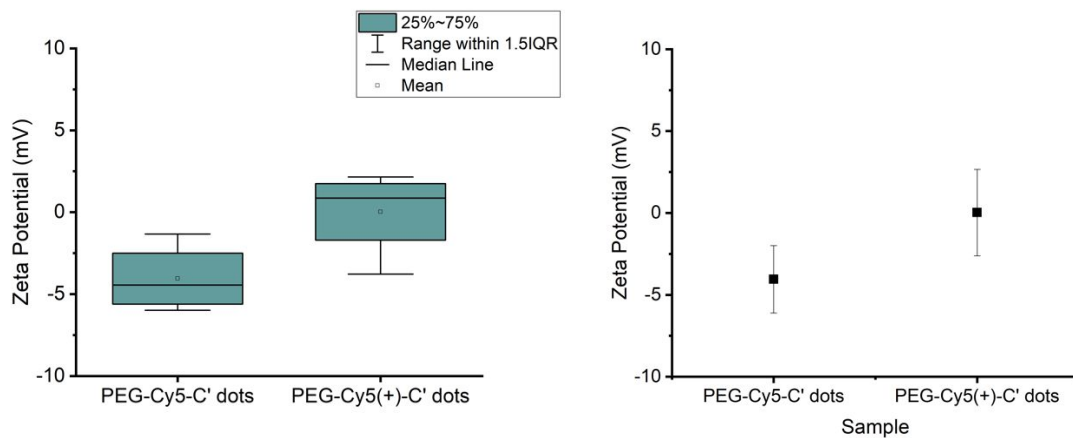


Figure S11: (A) Box and whisker plot comparison of zeta potential measurements on conventional PEG-Cy5-C' dots and improved PEG-Cy5(+)-C' dots. (B) The same data represented as a simple scatter plot. For each data point five measurements were averaged.

Sample	Diameter (nm)	Dyes/Particle (#)	Photoisomerization <i>P</i> (%)	Brightness/Dye (kHz)
Cy5 (free dye)	1.3	1.0	43.2	7881
PEG-Cy5-C' dots	5.8	1.6	35.2	17443
PEG-Cy5-C' dots Peak 1	5.6	1.5	33.2	18203
PEG-Cy5-C' dots Peak 2	5.8	2.0	37.8	14203
PEG-Cy5-C' dots Peak 3	5.7	2.3	41.3	12424
PEG-TMR-C' dots	6.4	3.6	-	-
PEG-ATTO647N-C' dots	6.2	2.0	-	-
PEG-ATTO680-C' dots	7.0	1.4	-	-
PEG-MB2-C' dots	4.3	2.6	-	-
cRGDyC-PEG-Cy5-C' dots	6.1	2.1	-	-
PEG-Cy5(+)-C' dots	5.9	1.5	-	-
cRGDyC-PEG-Cy5(+)-C' dots	6.0	-	-	-

Table S1: Particle size and dyes per particle of the various C' dots used in the study. For samples subjected to after pulse corrected fluorescence correlation spectroscopy, photoisomerization and brightness per dye is also tabulated.

Peak Number	Retention Time (min)	Area (%)
1	5.784	0.59
2	8.622	82.08
3	10.477	5.68
4	20.704	4.22
5	23.231	7.42

Table S2: Peak integration areas and retention times for native synthesis solution of PEG-TMR-C' dots shown in Figure S4 as determined by Empower3 software using the ApexTrack peak detection algorithm. Corresponding peaks are labeled in Figure S4.

Peak Number	Retention Time (min)	Area (%)
1	9.037	62.11
2	11.946	7.45
3	13.412	30.44

Table S3: Peak integration areas and retention times for native synthesis solution of PEG-Cy5-C' dots shown in Figure S5 as determined by Empower3 software using the ApexTrack peak detection algorithm. Corresponding peaks are labeled in Figure S5.

Peak Number	Retention Time (min)	Area (%)
1	8.87	100

Table S4: Peak integration area and retention time for native synthesis solution of PEG-ATTO647N-C' dots shown in Figure S6 as determined by Empower3 software using the ApexTrack peak detection algorithm.

Peak Number	Retention Time (min)	Area (%)
1	30.940	27.68
2	31.779	37.70
3	32.725	28.65
4	33.785	5.96

Table S5: Peak integration areas as determined with ApexTrack integration in Empower 3 for the HPLC chromatogram of PEG-Cy5-C' dots at 647 nm as shown in Fig. 1B.

Peak Number	Retention Time (min)	Area (%)
1	30.940	52.35
2	31.779	14.18
3	32.725	20.5
4	33.785	12.89

Table S6: Peak integration areas as determined with ApexTrack integration in Empower 3 for the HPLC chromatogram of PEG-Cy5-C' dots at 275 nm as shown in Fig. 1B.